Interpretation of the variability of the Cephei star Scorpii. I. The multiple character

Journal Item

A&A 427, 581–592 (2004)
DOI: 10.1051/0004-6361:20041223

Astronomy & Astrophysics

Interpretation of the variability of the β Cephei star λ Scorpii

I. The multiple character⋆,⋆⋆

K. Uytterhoeven[1,2], B. Willems[3,4], K. Lefever[1], C. Aerts[1,5], J. H. Telting[6], and U. Kolb[4]

[1] Institute of Astronomy, Catholic University Leuven, Celestijnenlaan 200 B, 3001 Leuven, Belgium
e-mail: katrien.uytterhoeven@ster.kuleuven.ac.be
[2] Mercator Telescope, Calle Alvarez de Abreu 70, 38700 Santa Cruz de La Palma, Spain
[3] Department of Physics and Astronomy, Northwestern University, 2145 Sheridan Road, Evanston, IL 60208, USA
[4] Department of Physics and Astronomy, The Open University, Milton Keynes, MK7 6AA, UK
[5] Department of Astrophysics, University of Nijmegen, PO Box 9010, 6500 GL Nijmegen, The Netherlands
[6] Nordic Optical Telescope, Apartado de Correos 474, 38700 Santa Cruz de La Palma, Spain

Received 4 May 2004 / Accepted 15 July 2004

Abstract. We derive accurate values of the orbital parameters of the close binary β Cephei star λ Scorpii. Moreover, we present the first determination of the properties of the triple system to which λ Scorpii belongs. Our analysis is based on a time series of 815 high-resolution spectra, covering a timespan of 14 years. We find a close orbit of $5\overset{\mathrm{d}}{.}9525$ days ($e = 0.26$) and a wide orbit of approximately 1082^{d} days ($e = 0.23$). The orbital parameters of the triple star and a spectrum synthesis lead us to conclude that the system is composed of two early-type B stars and a low-mass pre-main-sequence star rather than containing an ultra-massive white dwarf as claimed before. Our proposed configuration is compatible with population synthesis. The radial velocity variations of the primary allow us to confirm the presence of at least one pulsation mode with frequency 4.679410 c d^{-1} which is subject to the light-time effect in the triple system. A detailed analysis of the complex line-profile variations is described in a subsequent paper.

Key words. stars: binaries: spectroscopic – stars: binaries: close – stars: oscillations – line: profiles – stars: individual: λ Scorpii

1. Introduction

Several pulsating B-stars turn out to be components of multiple systems. From the sample of known B-type line-profile variable stars one can work out that all broad-lined stars show moving "bumps" and that many of these objects are members of a close binary. Since a companion might have an effect on the pulsation of the star due to tidal interactions, the following, still unanswered, question is: does binarity and/or rotation play a role in pulsation-mode selection and/or in the enhancement of pulsation-mode amplitudes?

From a theoretical point of view tidal effects can induce forced oscillations (e.g. Cowling 1941) or alter free oscillations (e.g. Kato 1974; Reyniers & Smeyers 2003a,b). Witte & Savonije (1999a) have shown from theoretical calculations that tidally excited gravity-mode oscillations in rotating massive stars are a means to dissipate orbital energy at high rates, if the disturbing orbital frequency coincides with a resonance frequency of the star. Thus, the tidally excited pulsations may have an impact on binary star evolution. Smeyers et al. (1998) developed a formalism to describe the displacement field associated with resonant dynamic tides which was subsequently used by Willems & Aerts (2002) to derive the tidally induced radial velocity (RV) variations in close binary components. The latter authors pointed out that, depending on orbital eccentricity and on orbital inclination, the amplitude of RV variations induced by tidal interactions can be large enough to be detected by observers. As an example they analysed the slowly pulsating B star HD 177863 ($P_{\mathrm{orb}} = 12^{\mathrm{d}}, e = 0.60$) of which De Cat & Aerts (2002) reported a nonradial pulsation (NRP) mode with a frequency equal to 10 times the orbital frequency, and found a possibility of resonant excitation of a g-mode.

In general, not many observational cases with firm evidence of tidally excited oscillations are known. Until now there exist only two objects with convincing evidence: the star HD 177863 mentioned above and the hybrid γ Doradus star HD 209295 (Handler et al. 2002) which is a close binary with high eccentricity ($P_{\mathrm{orb}} = 3\overset{\mathrm{d}}{.}1, e = 0.35$) whose intrinsic variations

⋆ Based on observations obtained with the Coudé Echelle Spectrograph on the ESO CAT telescope and with the CORALIE Echelle Spectrograph on the 1.2-m Euler Swiss telescope, both situated at La Silla, Chile

⋆⋆ Table 1 is only available in electronic form at http://www.edpsciences.org

show several frequencies that are exact integer multiples of the orbital frequency. Other good candidate stars for tidally excited pulsation modes are σ Scorpii ($P_{\rm orb} = 33^{\rm d}, e = 0.40$, Fitch 1967), α Virginis ($P_{\rm orb} = 4^{\rm d}, e = 0.15$, Smith 1985a,b), ψ^2 Orionis ($P_{\rm orb} = 2\overset{\rm d}{.}53, e = 0.05$, Telting et al. 2001) and ν Centauri ($P_{\rm orb} = 2\overset{\rm d}{.}62, e = 0.0$, Schrijvers & Telting 2002). The small number of confirmed cases might be due to a lack of systematic observational studies dedicated to the problem.

A few years ago Harmanec et al. (1997) set up the observational project SEFONO (SEarch for FOrced Nonradial Oscillations) with the aim of making a systematic search for line-profile variations (LPVs) in the early-type primaries of known, short-period binary systems and to study orbital forcing as possible source of NRP. Our observational study of tidal interactions on NRP modes takes a different complementary approach. Our starting point is a sample of selected B-type stars that are known to be non-radial pulsators and that turn out to be close binaries. For each member of this sample we aim to obtain a sufficiently large dataset of high S/N, high-resolution spectra to perform a detailed study of the LPVs. Additionally we may be able to distinguish oscillations of a forced nature. From the results of the whole sample we finally hope to lift a corner of the veil that is covering the enhancement of pulsation modes by tidal forces. A first outline of this project is given by Aerts et al. (1998).

In the framework of our project we report the results for the β Cephei star λ Scorpii. The whole analysis is presented in two papers. The second paper (Paper II, Uytterhoeven et al. 2004) describes the results of a detailed analysis of the frequency spectrum and of the investigation of the presence of tidally induced pulsation modes. In the current paper we solve the triple system and derive its orbital parameters. Section 2 gives an overview of the current knowledge of λ Scorpii. In Sect. 3 we present our dataset. Section 4 is devoted to the derivation of the orbital motion of both the close orbit and the triple system from our spectra. It also contains a brief study of the intrinsic variations in the RV changes and an analysis of the HIPPARCOS light curve. This allows us to derive the physical nature of the triple system. Our model is subsequently confronted with a population synthesis of the close binary in Sect. 5 and with line-profile synthesis in Sect. 6. This allows us to conclude our description of the nature of the three components in a final Sect. 7.

2. The target star λ Scorpii

The star λ Scorpii (HD 158926, HR 6527, 35Sco, $\alpha_{2000} = 17^{\rm h}33^{\rm m}36\overset{\rm s}{.}52$, $\delta_{2000} = -37°06'13.8''$, $m_V = 1.62$) is listed as a B2IV+B system in the Bright Star Catalogue (Hoffleit 1982). It is located at a distance of approximately 216 ± 42 pc (HIPPARCOS catalogue, Perryman et al. 1997), and is one of the brightest massive stars in the southern hemisphere.

The star has been the subject of several earlier RV and photometric studies. Slipher (1903) discovered the star to be a spectroscopic binary. Additional studies of the close binary system were performed by Lomb & Shobbrook (1975) and Lesh & Aizenman (1978). The orbital period listed by these authors ranges from 5.6 to 10.2 days. De Mey et al. (1997) first studied the orbital motion of the close binary in detail and reported changes in the gamma-velocity as well, leading to the suggestion that it concerns a triple system. These authors determined the period of the eccentric orbit with much higher precision than before and obtained $5\overset{\rm d}{.}96$. They had insufficient coverage to derive the elements of the triple system. Based on interferometric techniques, Hanbury Brown et al. (1974) claimed λ Scorpii to be a visual binary consisting of two B stars with almost equal brightness and colour. On the other hand, Berghöfer et al. (2000) gave an entirely different view of the nature of the companion of λ Scorpii. They explain the soft X-ray emission, detected with the Einstein Observatory (Giacconi et al. 1979) and ROSAT satellite (Trümper 1983), in terms of an ultra-massive white dwarf companion, using the (uncertain) mass function of the close binary derived by De Mey et al. (1997). The nature of this object therefore remains unclear.

As for the intrinsic variability of the primary, Shobbrook & Lomb (1972) and Lomb & Shobbrook (1975) used long-term photometric and RV observations obtained between 1969 and 1973 and classified the star as a new β Cephei variable. They reported a dominant period of $P_1 = 0\overset{\rm d}{.}2137015$ in combination with its first harmonic $P_2 = 0\overset{\rm d}{.}10685075$. Watson (1988), treating the system as a single star, interpreted the variability with P_1 in terms of a radial oscillation. De Mey et al. (1997) confirmed the line-profile variable character of λ Scorpii as first detected by Waelkens (1990). Their analysis of 3 nights of high-resolution spectra obtained in June 1995 revealed only one pulsation frequency $f_1 = 4.66$ c d^{-1}, which is compatible with the first period found by Lomb & Shobbrook (1975). Although a profound mode identification could not be performed due to the too large scatter in the velocity moments, De Mey et al. (1997) explained this frequency in terms of NRP and found indications for the presence of more than one mode.

Given the brightness of the star, its physical parameters have been determined in several studies, each time with the assumption of a single star. Lomb & Shobbrook (1975) use $R = 9 \pm 1\ R_\odot$, $\log T_{\rm eff} = 4.371$ and $\log g = 3.5$. Westin (1985) lists $\log T_{\rm eff} = 4.353$ while Gulati et al. (1989) list $\log T_{\rm eff} = 4.444$. Heynderickx et al. (1994) determined the physical parameters from calibrations of different photometric systems and obtained $\log T_{\rm eff} = 4.326$, $\log g = 3.768$, $M = 10.81\ M_\odot$, $M_{\rm bol} = -5.15$ from Strömgren photometry and $\log T_{\rm eff} = 4.364$, $\log g = 3.755$, $M = 10.50\ M_\odot$, $M_{\rm bol} = -5.53$ from Geneva photometry. These results suggest a radius of $R \approx 7\ R_\odot$. Berghöfer et al. (1996) obtained $\log L_{\rm bol} = 37.72$ and $\log L_{\rm X} = 30.26$. Finally, Pasinetti Fracassini et al. (2001) give the constraint $6.5\ R_\odot \leq R \leq 7.0\ R_\odot$.

In the literature we find different values of the projected rotational velocity $v \sin i$: 163 km s^{-1} (Hoffleit 1982), 120 km s^{-1} (Watson 1971), 250 km s^{-1} (Buscombe 1969); 157 km s^{-1} (Stoeckley & Buscombe 1987), 145 km s^{-1} (De Mey et al. 1997) and 150 km s^{-1} (Brown & Verschueren 1997). The latter authors listed λ Scorpii as a probable member of the Upper Scorpius (US) OB2 association. Assuming this membership, Berghöfer et al. (2000) estimated the age of λ Scorpii to be between 13 and 18 Myr. This estimate is based on the age of the single B-type star ν Scorpii which is supposed to belong to the US association and thus probably formed under

the same conditions and around the same time as λ Scorpii. However, we have to be cautious with both age estimation and assumed membership as de Zeeuw et al. (1999) did not include λ Scorpii in the list of confirmed members of the US association after an investigation of HIPPARCOS positions, proper motions and parallaxes of candidate members of OB2 associations. Moreover, when we compare the galactic coordinates of λ Scorpii with the position of OB associations as can be found in the paper, we find that λ Scorpii lies closer to the Upper Centaurus Lupus association (UCL) than to the US association. De Zeeuw et al. (1999) estimate the distances to the US and UCL associations to be 145 pc respectively 140 pc and report an age between 5 and 6 Myr for the US association, and an age between 14 and 15 Myr for the UCL association. This age estimation of the US association is very different from the one assumed by Berghöfer et al. (2000). Another attempt to estimate the age of λ Scorpii was made by De Mey et al. (1997). They derived an age of 20 to 28 Myr by fitting theoretical stellar models to the observed luminosity and effective temperature. We note, however, that such a procedure is highly inaccurate as it does not account for interactions between the binary components, which are not unlikely to have occurred, given the short orbital period (see also Sect. 5.3).

3. Data and data reduction

With our sights set on a detailed study of the orbital motion and the pulsational behaviour, two observing programmes were dedicated to the project of λ Scorpii. The first programme concerned intensive monitoring of the star during eight consecutive nights in order to study the pulsational behaviour. The idea behind the second programme was the gathering of additional spectra, well spread in time, in addition to the dataset described by De Mey et al. (1997), to obtain a dataset with a large time base to unravel the triple system.

3.1. CAT/CES spectra

The intensive monitoring resulted in an extensive dataset of high-resolution ($55\,000 \leq R \leq 60\,000$) and high signal-to noise ($S/N > 400$) spectra, gathered with the CAT telescope and the CES spectrograph at ESO, La Silla, during eight consecutive nights in July 1997. We used CCD#38, which is a Loral/Lesser 2688×512 pixel CCD with a pixel size of 15×15 μm^2. The spectral domain was centered on the Si III triplet at 4552.654 Å, 4567.872 Å and 4574.777 Å. The integration times were between 45 s and 4 min, which is less than 1.5% of the known main period of the intrinsic variation. A logbook of the eight nights is given in the bottom panel of Table 1. This table is only available in the electronic version of the paper. The logbook contains information about the Julian date of the observations, the number of spectra obtained, the mean S/N and the mean integration time expressed in seconds.

As part of our long-term observational programme of λ Scorpii, a few CAT/CES spectra were taken during the months March, May, July and October 1997. Information on the month and year of the observations, the number of spectra obtained and the range in signal-to-noise (S/N) ratio, is listed in the upper part of Table 1 (labelled with $\star$).

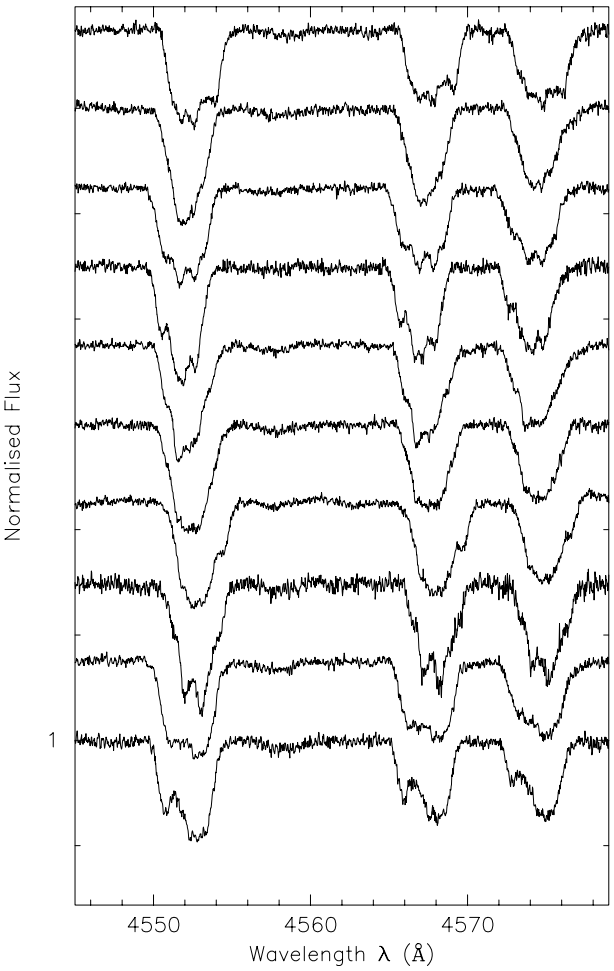

Fig. 1. A randomly chosen set of reduced spectra of λ Scorpii obtained in July 1997, focussed on the Si III triplet, showing the line-profile variations due to pulsation.

We used the ESO-Midas software package for the reduction of the spectra. After subtracting a mean bias-value, we removed the pixel-to-pixel sensitivity variations inherent in the detector by flatfielding with spectra of a quartz flatfield lamp. We continued the reduction procedure by means of a wavelength calibration using the spectra of a ThAr lamp. We rebinned all spectra such that $\Delta\lambda = 0.02$ Å and used a cubic spline function to perform the continuum normalisation. Finally, all spectra were shifted to the heliocentric frame.

For illustration, an arbitrarily chosen set of reduced spectra gathered in July 1997 is shown in Fig. 1. It is clear that λ Scorpii is a broad-lined star, which shows "bumps" moving through the profiles. Visual inspection does not provide evidence of any absorption lines of the other components of the system in the Si III lines.

3.2. Euler/CORALIE spectra

In order to study the orbital motion in the triple system, we used the CORALIE échelle spectrograph on the 1.2-m Euler

Table 2. Overview of the different orbital period, derived by different authors.

Author(s)	$P_{\rm orb}$
Slipher (1903)	$5\overset{\rm d}{.}6$
Lomb & Shobbrook (1975)	$\sim 10^{\rm d}$
Lesh & Aizenman (1978)	$10\overset{\rm d}{.}16$
De Mey et al. (1997)	$5\overset{\rm d}{.}959$
Uytterhoeven et al. (this paper)	$5\overset{\rm d}{.}9525$

Swiss telescope at La Silla to obtain additional spectra. A logbook of the measurements is given in Table 1. The observations are labelled with °. The wavelength domain of the CORALIE fiber-fed spectrograph ranges from 3875 to 6820 Å recorded on 68 orders. The CCD camera is a 2k × 2k CCD with pixels of 15 μm. CORALIE reaches a spectral resolution of 50 000 with a 3 pixel sampling. The S/N ratio of the obtained CORALIE spectra varied between $S/N = 100$ and $S/N = 210$.

An on-line reduction of the CORALIE spectra, using the INTER-TACOS software package, is available. For a description of the reduction process we refer to Baranne et al. (1996). We did a more precise correction for the pixel-to-pixel sensitivity variations by using all available flatfields obtained during the night instead of using only one flatfield, as is done by the on-line reduction procedure. The normalisation of the spectra and the heliocentric correction were carried out using the ESO-Midas software package, following the same procedure as for the CAT spectra. For an accurate merging of the different échelle orders, we followed the procedure as described by Erspamer & North (2002).

4. The orbital motion

Several attempts to determine the orbital period were performed by different authors (see Sect. 2). An overview of the orbital periods is given in Table 2. De Mey et al. (1997) found evidence for the presence of a third component because there are seasonal variations of the velocity of the center of mass of the binary. The orbital motion of this third component has not yet been studied in detail; a time span of a few months or even years is required to do so. The total dataset we present here spans a period of more than 5000 days (see Table 1) and should allow us to determine the period of the wide system.

4.1. Radial velocities

Because of the distortions of the line profiles due to the moving "bumps", Gaussian fits were not accurate enough to calculate the RVs. Therefore we derived the RVs of the CAT spectra by means of the centroid of the first and second Si III line at 4552.654 Å and 4567.872 Å, according to the definition of the first moment of the line given in Aerts et al. (1992). This requires the determination of the position of the continuum on either side of the line. The movement of the absorption line of the primary due to binarity made it impossible to use fixed integration boundaries for each spectrum, so we determined the boundaries for each spectrum individually.

The higher noise level of the CORALIE data caused a large scatter in the RVs. To reduce the scatter, we computed the RVs by cross-correlating the lines in the observed spectra with those of a numerical template following Baranne et al. (1996). The numerical template spectrum was derived from a Kurucz atmosphere model with $T_{\rm eff} = 22\,000\ K$ and $\log g = 4.0$.

To analyse the close binary and triple system we made use of two different FORTRAN codes. The first one, called VCURVE, calculates the best-fitting set of orbital parameters of a binary system from RV measurements using the Léhmann-Filhés method (1894). The second code, FOTEL, allows separate or simultaneous solutions of light- and RV-curves of binary stars and/or triple stars (Hadrava 1990).

The analysis was carried out on the RV datasets calculated from the Si III 4552.654 Å and the Si III 4567.872 Å profiles, and also on the mean RVs obtained from these two silicon lines of all spectra listed in Table 1. We note that, due to vignetting, the bluest silicon line was not available for the spectra obtained during one night in June 1995 (44 spectra).

On the one hand we used VCURVE to obtain an orbital solution of the triple system. Since VCURVE can only handle a binary system, we worked in different stages. First, we determined the best-fitting orbital solution of the close binary system. Subsequently, we removed the influence of this short orbit from the data and searched for the orbital solution of the long orbit in the residual dataset. In an iterative process we refined the orbital solution of the close binary system by first removing the influence of the long orbit from the original data before searching for the short orbit, followed by a new search for the long orbit after removal of the refined short orbit from the original data. This iterative process turned out to be necessary as the velocity shift due to the long orbit distorts the RV distribution, and hence the value of the best-fitting orbital parameters of the short orbit. The effect of this distortion is shown in the top panel of Fig. 2: datapoints at minimum (maximum) velocity in the long orbit have a negative (positive) velocity shift and are located relatively lower (higher) in the phase diagram of the short orbit. On the other hand we searched for a best-fitting solution of the triple system by solving the three-body problem by means of FOTEL. For both methods we assigned weights to each datapoint scaled with the S/N ratio of the observed spectrum.

Analysis of the different sets of RVs by means of VCURVE and FOTEL resulted in an orbital period of the close system of $P = 5\overset{\rm d}{.}9525$, entirely compatible with the result obtained by De Mey et al. (1997). The orbital elements calculated from the mean RVs of the two bluest silicon lines using the two different codes are listed in Table 3. As one can notice, VCURVE and FOTEL deliver very similar results. We find an orbital period of the wide system of $P_2 = 1082^{\rm d} \pm 3^{\rm d}$, which is approximately 182 times longer than the orbital period of the close system. The orbital parameters of the wide orbit are also listed in Table 3.

Figure 2 shows the phase diagrams of the original RVs (dark gray dots) with respect to the orbital periods of $P_1 = 5\overset{\rm d}{.}9525$ and $P_2 = 1082^{\rm d}$ as presented in Table 3. Treating the triple system as two separate two-body problems in an iterative process (VCURVE) or treating it as a three-body problem

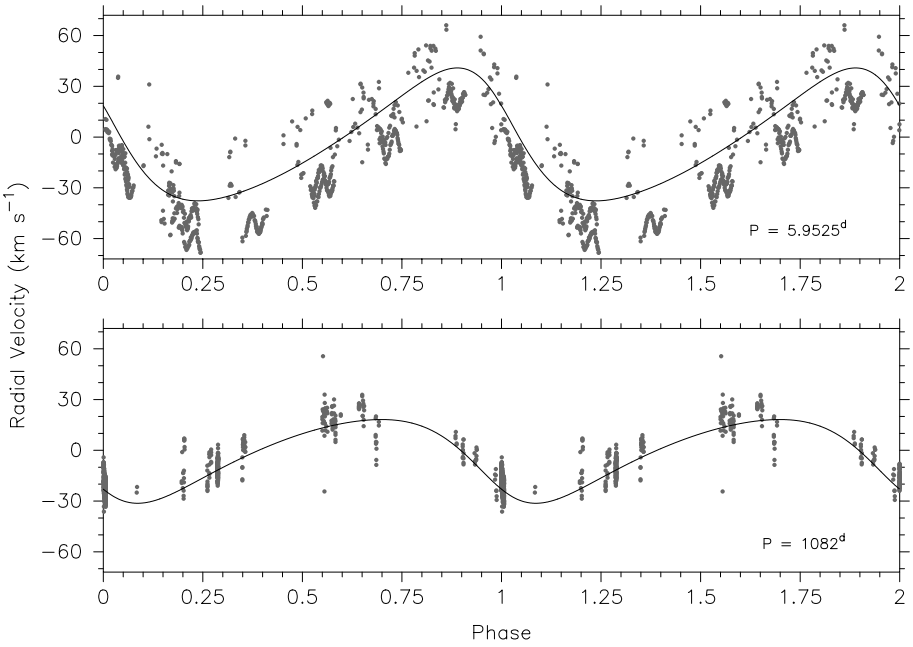

Fig. 2. Phase diagrams of the mean RVs with respect to the orbital periods of $P_1 = 5\overset{d}{.}9525$ (*top*) and $P_2 = 1082^d$ (*bottom*). The observed RVs are given by dark-gray dots. The orbital solutions obtained with FOTEL (Table 3) are represented by the black lines. The scattered distribution of the RVs in the upper plot is caused by the contribution of the long orbit. $\phi = 0$ corresponds to the epoch of periastron HJD 2 450 659 and 2 451 732 for the close, respectively wide orbit.

Table 3. The orbital parameters of λ Scorpii together with their rms error derived from mean RVs of the 4552.654 Å and 4567.872 Å line of all spectra listed in Table 1 by using VCURVE (second column) and FOTEL (third column).

Orbital parameter	VCURVE	FOTEL
$P_{\rm orb,close}$ (days)	$5.95254 \pm 4 \times 10^{-5}$	$5.95254 \pm 6 \times 10^{-5}$
$v_{\gamma,\rm close}$ (km s^{-1})	1.1 ± 0.4	–
$K_{\rm close}$ (km s^{-1})	39.3 ± 0.2	39.3 ± 0.4
$E_{0,\rm close}$ (HJD)	$2\,450\,659.27 \pm 0.02$	2450659.27 ± 0.03
$e_{\rm close}$	0.26 ± 0.01	0.26 ± 0.01
$\omega_{\rm close}$ (degrees)	64 ± 3	65 ± 2
$a_1 \sin i_{\rm close}$ (AU)	0.0208 ± 0.0003	0.0208 ± 0.0002
$f(M)_{\rm close}$ ($M_\odot$)	0.034 ± 0.001	0.0336 ± 0.0009
$P_{\rm orb,wide}$ (days)	1083 ± 3	1082 ± 3
$v_{\gamma,\rm wide}$ (km s^{-1})	2.1 ± 0.2	–
$K_{\rm wide}$ (km s^{-1})	23.6 ± 0.6	24.7 ± 0.4
$E_{0,\rm wide}$ (HJD)	$2\,451\,695 \pm 25$	$2\,451\,732 \pm 29$
$e_{\rm wide}$	0.25 ± 0.02	0.23 ± 0.03
$\omega_{\rm wide}$ (degrees)	299 ± 10	311 ± 11
$a_1 \sin i_{\rm wide}$ (AU)	2.3 ± 0.05	2.39 ± 0.04
$f(M)_{\rm wide}$ ($M_\odot$)	1.33 ± 0.09	1.52 ± 0.07
$v_{\gamma,\rm total}$	–	-2.8 ± 0.4

(FOTEL, black line in Fig. 2) ended up in compatible orbital parameters. The observed RV changes of λ Scorpii (black dots) are plotted against the RV changes as predicted by the FOTEL triple solution (dark gray lines) in Fig. 3.

4.2. The intrinsic variations of the primary

As can been seen in Fig. 4, besides seasonal and weekly variations, the RVs of λ Scorpii also show nightly variations. The dataset of 421 high-resolution and high-S/N spectra of July 1997 was taken specifically with the aim to study the pulsational behaviour of the primary of the multiple system λ Scorpii (hereafter shortly called λ Scorpii) in full detail. Here, we focus only on the analysis of the intrinsic variations by means of the RV variations. For a detailed analysis of additional line diagnostics we refer to Paper II.

We studied the intrinsic variations of λ Scorpii based on all spectra of good quality and with an S/N ratio higher than 100. This dataset, consisting of 748 spectra and covering a time-span of more than 5000 days, enabled us to find intrinsic frequencies with high accuracy. To study the intrinsic variations we shifted the profiles to correct for both the short and wide orbital velocity. Subsequently, we calculated, for each spectrum, the first normalised moment $\langle v \rangle$ of the two bluest Si III lines, which is the line-centroid velocity (see also Sect. 4.1).

We used different frequency analysis methods on the centroids: Phase Dispersion Minimisation (PDM, Stellingwerf 1978), the Lomb-Scargle method (Scargle 1982) and the CLEAN algorithm (Roberts et al. 1987). For the PDM method we used the bin- and cover structures (5, 2) and (10, 3); for the CLEAN algorithm we used gain values 0.2 and 0.8. We searched for frequencies between 0 and 15 c d^{-1}, with frequency steps of 10^{-6} c d^{-1}. We found a dominant variation in the RVs with a frequency $f = 4.676672$ c d^{-1} (Si III 4552.654 Å), respectively 4.676685 c d^{-1} (Si III 4567.872 Å), with a peak-to-peak variation of about 10 km s^{-1}. Within the accuracy of our frequency determination the frequency f is a one year alias of 4.67942 c d^{-1} (Shobbrook & Lomb 1972; Lomb & Shobbrook 1975). Indeed, adding the highest peak in the window function to f leads to $f_1 = 4.679410$ c d^{-1}. Given that the time spread of the

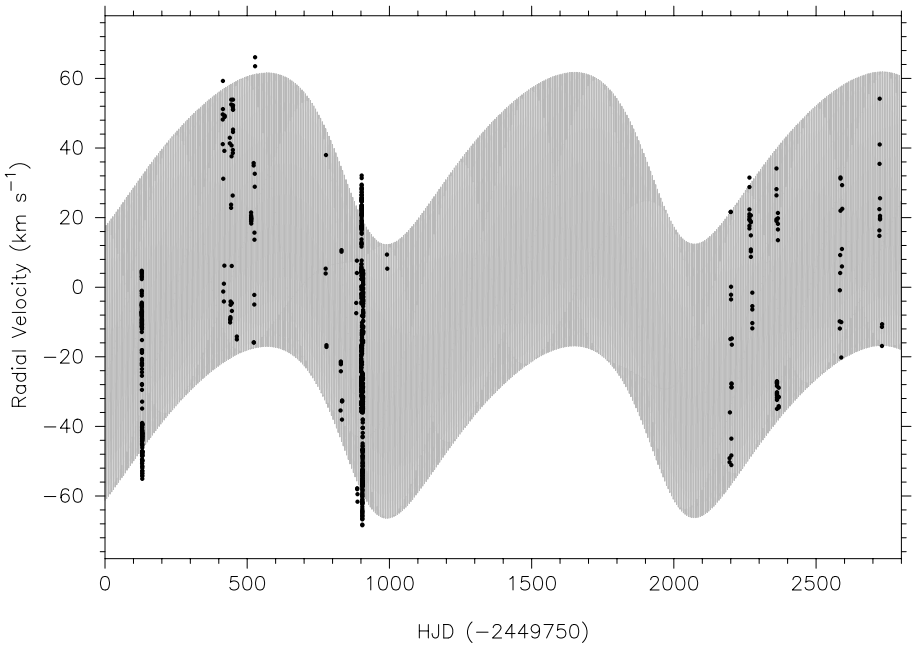

Fig. 3. Observed RVs obtained between June 1995 and July 2002 (black dots) together with the best solution of the triple system from FOTEL (dark gray line, see Table 3).

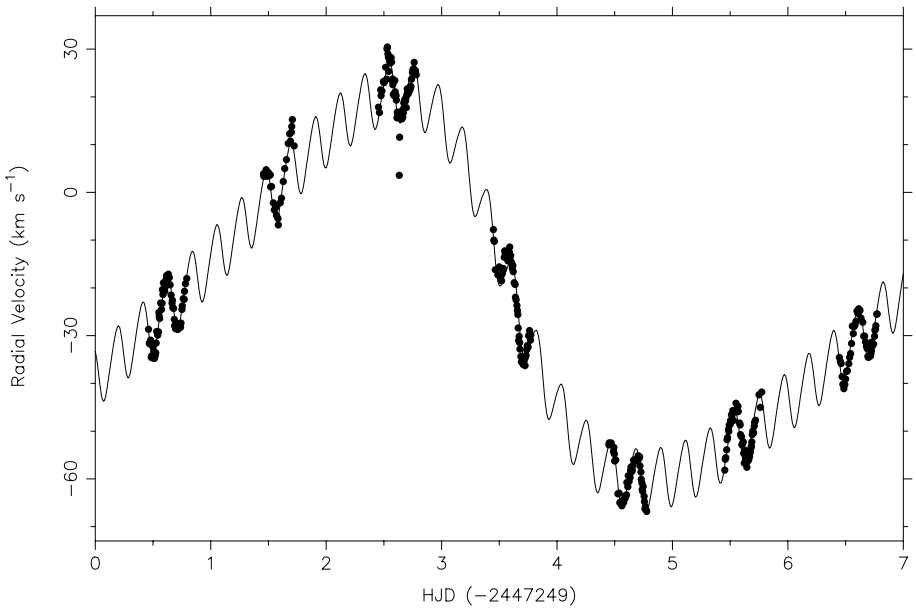

Fig. 4. RVs of λ Scorpii from the 421 spectra taken in July 1997. The combination of the FOTEL triple orbit and the main intrinsic variation with frequency f_1 is shown by the full line.

photometric data is better suited to disentangle the alias patterns, we accept f_1 as the true main intrinsic frequency. Figure 4 shows the radial velocity curve for the July 1997 data. The orbital solution to which the nightly changes in RV due to the main pulsation with frequency f_1 are added, is represented as a full line.

After prewhitening with f_1, similar frequencies with a value near f_1 show up again in the periodogram ($f \in [4.671; 4.698]$ c d^{-1}). This is surely a confirmation of the remark made by Lomb & Shobbrook (1975) that the dominant pulsation frequency of λ Scorpii is variable in time, with a variable amplitude. In fact, Lomb & Shobbrook (1975) had already noticed that the main frequency seems to vary cyclically with a period of about 3 years, which happens to coincide with the period of the wide orbit. Moreover, the variation of the frequency reported by Lomb & Shobbrook (1975, see their Fig. 5) is entirely compatible with it being caused by the light-time effect in the combined close and wide orbit according to the

amplitude we find for it and by considering $f_{1,\mathrm{true}} = f_{1,\mathrm{apparent}}(1 + \mathrm{Vrad}/c)$. The time spread of our spectroscopic data is unfortunately insufficient to derive detailed frequency changes as a function of time, as Lomb & Shobbrook (1975) were able to do (see also Paper II). However, the photometric results leave no doubt that also for our spectroscopic dataset the intrinsic frequencies should be affected by the light-time effect.

At present we do not exclude the presence of additional intrinsic frequencies besides f_1 with amplitudes near the noise level, but we refer to Paper II for a more detailed analysis of all the line diagnostics. See also the remarks made in Sect. 6.

4.3. The HIPPARCOS lightcurve

Shobbrook & Lomb (1972) found evidence for the occurrence of an eclipse with a depth of ~4 mmag in their lightcurve of λ Scorpii. If this were confirmed it would allow us to limit the inclination of the short orbit to a narrow range. To check this possibility we looked at the HIPPARCOS lightcurve of the star. In Fig. 5 we show the HIPPARCOS data with quality label 0, 1, 2 phased with the close orbit. We indeed find evidence for an eclipse near phase 0.1, which represents a magnitude increase of some 4 mmag and consists of data points from two different nights separated by 494 days. This is an independent indication that the phenomenon observed by Shobbrook & Lomb (1972) might indeed have been the primary eclipse of the star. As a consistency check we calculated the theoretically predicted ephemeris for the eclipses and find phase 0.11 for the primary and phase 0.76 for the secondary eclipse. Hence the observed decrease in light near phase 0.1 may indeed find its origin in the eclipse of the primary by the secondary. Unfortunately no observations were made near the predicted phase of the secondary eclipse, i.e. when the primary passes in front of the secondary.

If we phase the HIPPARCOS data with the period of the wide orbit, we do not see any dips in magnitude besides those resulting from the eclipse in the close orbit. This would tend to indicate that the primary and tertiary do not eclipse each other in the wide orbit. However, we do point out that the time spread of the HIPPARCOS data is only 783 days and the density of points is low. We hence take the conservative attitude that we cannot make a decision about the occurrence of eclipses within the wide orbit.

4.4. The mass functions

Since the mass function found in the present investigation is more than twice the value of 0.016 derived by De Mey et al. (1997), a re-evaluation of Berghöfer et al.'s (2000) interpretation that the secondary in the close binary is an ultra-massive white dwarf, is needed.

Assuming that we see an eclipse for the short orbit in the HIPPARCOS data, which is entirely compatible with Shobbrook & Lomb's (1972) observed eclipse and with the predicted ephemeris, and that the short orbit has a peak-to-peak variation of some 80 km s^{-1}, we can restrict the range of the inclination angle of the short orbit to $i_{\mathrm{close}} \geq 70°$. In Paper II we provide a totally independent estimate of the orbital

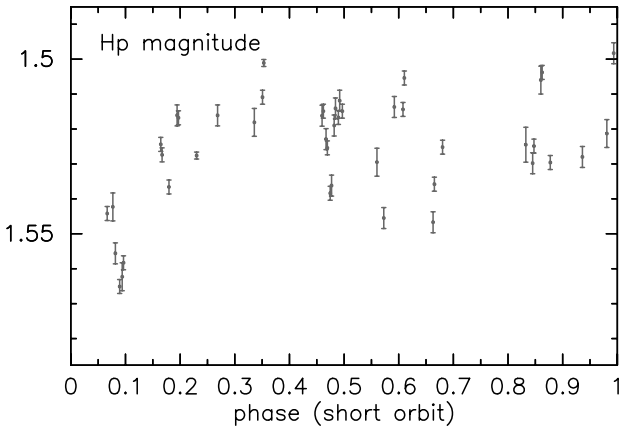

Fig. 5. HIPPARCOS data folded with the period of the close orbit (ϕ = 0 at HJD 2 447 921, epoch of periastron). Near phase 0.1 we see an increase in magnitude, corresponding to a decrease of the amount of observed light, most probably caused by an eclipse.

inclination angle from the identification of the main oscillation with frequency f_1. This leads to the interval $70° \leq i_{\mathrm{close}} \leq 90°$ assuming that the rotational and orbital inclination coincide. For a safe range of [10, 12] $M_\odot$ for the primary's mass, the mass function leads to a mass range of $M_2 \in [1.6, 2.0]$ $M_\odot$, which is much higher than the value obtained by Berghöfer et al. (2000) and also excludes a white-dwarf companion.

The high mass function of the wide orbit (see Table 3) subsequently leads to a range of [8.6, 9.6] $M_\odot$ for $M_3 \sin i_{\mathrm{wide}}$. The tertiary may therefore be a B star as well, with a mass that is only slightly lower than that of the primary. This would be entirely compatible with Hanbury Brown et al.'s (1974) proposal of a system consisting of two B stars of almost equal brightness. In Sect. 6 we find additional evidence for the B-type nature of the tertiary by means of a spectrum synthesis. Therefore we can exclude other possibilities such as, e.g., a stellar-mass black hole.

As the tertiary cannot be more massive than the primary we find that the inclination of the wide system cannot be lower than some 50°. This leads to mass estimates of the primary and tertiary B stars of respectively ~11 $M_\odot$ and ~9 $M_\odot$ with an uncertainty of about 1 $M_\odot$ for both estimates. We recall that the average mass estimate for the primary, assuming a single star, from Geneva and Strömgren photometry is 10.7 $M_\odot$.

5. Population synthesis

5.1. Basic assumptions

In order to further constrain the nature of the secondary in λ Scorpii from the point of view of binary evolution, we used the BiSEPS binary population synthesis code described by Willems & Kolb (2002, 2004). The code is based on the single star evolution formulae derived by Hurley et al. (2000) and follows all major phases of single and binary star evolution from the zero-age main sequence up to and including the remnant stages. The binary orbits are assumed to be circular and the rotation rates of the stars are assumed to be synchronised with

the orbital motion at all times. As the period of the orbit of the third B component is almost ~182 times as long as the period of the close binary, we here neglect its influence on the evolution of the close system. In particular, we do not consider the possibility that the third component became a member to the system in a tidal capture event which might have altered the orbital parameters of the inner binary at any point of its evolution. This limitation is not too restrictive in view of the relatively low stellar density in the Galactic field. Where appropriate, we will point out the caveats of this assumption when we discuss the system's possible evolutionary history (Sect. 5.3).

5.2. Initial parameters

We start the exploration of the evolutionary channels leading to λ Scorpii-type binary systems from a set of initial binaries with component masses ranging from 0.1 to 60 $M_{\odot}$, and orbital periods ranging from 0.1 to 10 000 days. A grid of 80 logarithmically spaced grid points was used for the initial masses of both the primary and the secondary component, and a grid consisting of 500 logarithmically spaced grid points was used for the initial orbital periods. For each binary, the evolution is followed up to a maximum age of 100 Myr or until it is destroyed. If one of the components undergoes a supernova explosion which leads to the birth of a neutron star, a set of 200 random kick velocities is generated from a Maxwellian velocity distribution with a dispersion of 190 km s^{-1}, and the evolution of the surviving binaries is followed until the imposed age limit.

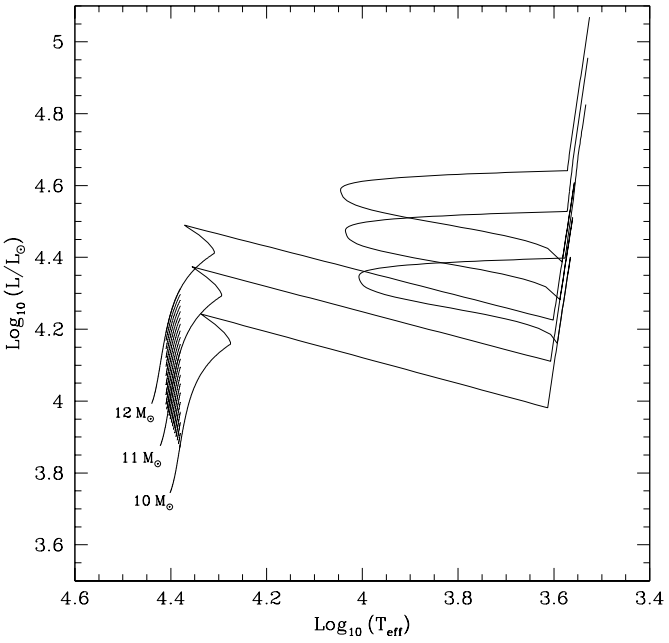

Fig. 6. Allowable parameter space in the Hertzsprung-Russell diagram for λ Scorpii-type primaries in our simulated samples of binaries. The evolutionary tracks are computed using the Single Star Evolution (SSE) code developed by Hurley et al. (2000). The main-sequence life times of the 10 $M_{\odot}$, 11 $M_{\odot}$, and 12 $M_{\odot}$ models are approximately 24 Myr, 21 Myr, and 18 Myr, respectively.

5.3. Results

Once we calculated the evolution of the binaries in our initial parameter grid, we scanned through the evolutionary tracks looking for systems with stellar and orbital parameters compatible with those of the close binary of λ Scorpii. In particular, we retained all systems which, at some point of their evolution, contain a main-sequence component with a mass between 10 $M_{\odot}$ and 12 $M_{\odot}$, a radius between 5 $R_{\odot}$ and 10 $R_{\odot}$, and an effective temperature between 24 000 K and 26 000 K. The corresponding region occupied by the primary in the Hertzsprung-Russell diagram is indicated by the hatched area in Fig. 6. We furthermore imposed the mass of the companion to be between 1.6 $M_{\odot}$ and 2.0 $M_{\odot}$ as derived above. To find appropriate matches for the orbital period in our simulated sample of binaries we first determine the orbital period λ Scorpii would have if it were circularised instantaneously. Conservation of the total orbital angular momentum of the binary then yields an orbital period of about 5.4 days. In our simulated samples of binaries we relax the orbital period constraint somewhat and consider all systems with an orbital period between 2 and 8 days in which the primary and secondary satisfy all imposed constraints as λ Scorpii-type binaries. Our calculations then result in three different evolutionary channels leading to binaries with stellar and orbital parameters compatible with those of λ Scorpii.

The first group of simulated λ Scorpii-type binaries consists of two main-sequence stars that have remained detached throughout their entire evolution. These systems typically have an age between 5 and 15 Myr, so that the primary has completed at least half of its evolution on the main sequence. This age range is in agreement with the age λ Scorpii would have if it belongs to and has the same age as the Upper Scorpius OB2 association. The high orbital eccentricity $e = 0.26$ may pose a problem for this formation channel though, since resonance lockings between dynamic tides and prograde g-modes are expected to circularise the orbits of such systems in only a few million years (Witte & Savonije 1999b). When the effects of resonances are neglected, circularisation is not expected to occur within the main-sequence lifetime of the B-type component (e.g. Zahn 1992). Hence, to settle the circularisation issue a more detailed exploration of this evolutionary channel by means of a full stellar and binary evolution code which takes into account the effects of dynamic tides is required. Such a treatment is however beyond the scope of the current exploration of possible evolutionary channels. We also note that the eccentricity of the inner binary may be subjected to slow large-amplitude oscillations caused by the presence of the third component (i.e. Kozai cycles; see, e.g., Eggleton & Kiseleva-Eggleton 2001).

The second group of simulated λ Scorpii-type systems consist of a main-sequence star accompanied by a naked-helium star. The progenitors of these systems are all subject to a dynamically unstable case B mass-transfer phase when the initially most massive star crosses the Hertzsprung gap or ascends the giant branch. The phase leads to the formation of a common envelope around the system in which tidal friction transfers

orbital energy of the component stars into rotational energy for the envelope (for a recent review on common envelope evolution, see Taam & Sandquist 2000). The spiraling-in of the binary components and the spin-up of the envelope lead to the expulsion of the envelope, leaving behind a binary with a period of the order of a few days consisting of a naked helium star (the helium core of the mass donor) and a main-sequence companion. The binary subsequently evolves through a λ Scorpii-type phase when the main-sequence component reaches the right evolutionary stage. Depending on the orbital separation after the common-envelope phase, the λ Scorpii-type phase may be preceded by a short mass-transfer phase from the naked-helium star to the main-sequence companion. The systems are typically between 15 and 30 Myr old, which is somewhat older than the age estimates for the Upper Scorpius OB2 association. Due to the strong tidal friction experienced by the binary components during the common-envelope phase, the naked-helium star + main-sequence star combination may also be hard to reconcile with the relatively high orbital eccentricity of λ Scorpii, unless it is caused by the interaction with the third component. The effective temperature of the naked-helium star in these systems ranges from 25 000 K to 35 000 K so that its signature should be detectable in the spectra. We come back to this in the next section.

The third group of simulated λ Scorpii-type systems consists of main-sequence stars with neutron star companions. The initial evolution of the systems is similar to that of the naked-helium star + main-sequence star binaries with the exception that the common-envelope phase of the initially most massive star can now take place on the asymptotic giant branch (case C mass transfer) as well as in the Hertzsprung gap or on the giant branch (case B mass transfer). The systems evolve through a phase comparable to the present configuration of λ Scorpii after the supernova explosion of the naked helium star, when the main-sequence component reaches the right evolutionary stage. If no mass transfer takes place from the helium star before it explodes as a supernova, the binaries typically have an age between 5 and 15 Myr. If mass transfer does take place, the age ranges from 20 to 30 Myr. The main advantage of this formation channel is that the occurrence of the supernova kick at the birth of the neutron star provides a natural explanation for the high orbital eccentricity of λ Scorpii. However, a clear caveat is the survival of the triple system during the supernova explosion of the primary in the close inner binary. Since the kick imparted to the neutron star at birth changes both the magnitude and the direction of the systemic velocity of the inner binary (for details see, e.g., Kalogera 1996), survival of the triple system may be difficult unless the kick is conveniently directed. In addition, the development of a common-envelope phase on the asymptotic giant branch requires large initial orbital separations corresponding to orbital periods of more than 1000 days, which is hard to reconcile with the presence of the third component in the wide 1082 day orbit. A possible solution might be that the third component was initially in an even wider orbit which shrunk to its present size due to the interaction with the envelope shed from the inner binary. Common-envelope phases from giant-branch donors pose less of a problem since they may already occur for binaries with periods substantially less than 1000 days. Finally, it is also interesting to note that, if the close companion of the B star in λ Scorpii is a neutron star, its mass has to be substantially larger than the canonical value of 1.4 $M_{\odot}$.

5.4. Summary

While the basic assumptions of our population synthesis are rather restricted given the neglect of the tertiary, we do end up with three likely scenarios for the companion in the close orbit: a low-mass (pre-) main-sequence star, a naked helium star or a neutron star. We now turn to a synthesis of the system's spectrum to come to a final most likely scenario.

6. Spectrum synthesis

We used the 18 CORALIE data obtained in February 2001, which cover the close orbit completely, to generate one high S/N ratio échelle spectrum. We did so by shifting each of the individual spectra of that run so that the RV derived from the cross-correlation function is placed at zero velocity, i.e. we shifted the profiles to the restframe of the primary. We note that this also implies that the radial velocities of the secondary and tertiary are considered in the restframe of the primary. Consequently, the averaged spectrum contains the intrinsically broadened profiles of the secondary and tertiary which are spread out over approximately 100 km s^{-1} due to the orbital movement. Subsequently, we focused on the regions where the Si II (4128 Å, 5050 Å), Si III (4560 Å, 4820 Å, 4716 Å, 5739 Å), Si IV (4116 Å, 4089 Å), He I (4026 Å, 4387 Å, 4471 Å, 4922 Å, 4713 Å, 6678 Å), He II (4686 Å), Hα, Hβ, Hγ, Hδ and Hϵ line profiles are expected.

Next we computed theoretical line profiles from spherically symmetric non-LTE atmosphere models by means of the newest version of the FASTWIND code (Fast Analysis of STellar Atmospheres with WINDs, Santolaya-Rey et al. 1997), which includes the effects of metal line blocking/blanketing (see Herrero et al. 2002) as well as a consistently calculated temperature structure based on the thermal balance of electrons, except for the innermost part of the atmosphere, where a flux-correction method is applied (see Kubat et al. 1999). The theoretical profiles are dependent on the parameters $T_{\rm eff}$, $\log g$, the microturbulent velocity and the particle number ratio N(He)/N(H). Especially the wings of the hydrogen lines and the ionisation balance between Si II, Si III, Si IV put strong constraints on respectively the gravity and the temperature of the star(s).

At first sight, we do not see any clear signature of the tertiary in the spectrum while the mass function leaves no doubt that it must be a B star, i.e. of similar spectral type to the primary. The wide orbit has a peak-to-peak velocity of some 50 km s^{-1}. Given that we had to use an overall broadening of some 140 km s^{-1} to fit the line profiles, we expect the lines of the tertiary to fall completely within those of the primary for most of the lines, assuming a not too large overall broadening of the tertiary. Moreover, the large rotational broadening of the primary implies severe blending of the lines in some regions of the spectrum.

A first firm conclusion is that only the He II 4686 Å line is observed in the spectrum while no other He II lines are seen. This excludes immediately that the secondary is a hot naked helium star. For the two other scenarios, i.e. a low-mass main-sequence star or a neutron star, we do not expect any signature of the secondary in the spectrum. Assuming that only the primary is responsible for the He II line implies that it must have a temperature in the range [24 000, 26 000] K. Further, except for the lines at 4089 Å and 4116 Å, which become visible for temperatures higher than 20 000 K, none of the Si IV lines are detected, which is what one would expect for this temperature range and the broadening of the primary. We next turn to the Si II lines. While the doublet at 4128 Å and 4130 Å is severely blended, it is clearly present and it has too high an equivalent width to be due to the primary alone. We therefore conclude that the tertiary makes a significant contribution to this doublet, which suggests a temperature range of [20 000, 22 000] K for a main-sequence star. We have merged theoretical spectra of the primary and tertiary for the appropriate flux ratios for combinations of the temperature ranges given above and $\log g \in [3.5, 4.0]$ for both stars. The best overall fits for all the lines mentioned above is obtained for a combination of two stars with solar helium composition and with $T_{\rm eff} = 25\,000$ K, $\log g = 3.8$ for the primary and $T_{\rm eff} = 22\,000$ K, $\log g = 4.0$ for the tertiary. This is entirely compatible with the results derived from the mass function of the wide orbit and leads us to conclude that the primary is a B1.5IV star and the tertiary a B2V star. Good fits required a broadening of 160 km s^{-1} for the tertiary and 140 km s^{-1} for the primary. We note here that an overall broadening of 160 km s^{-1} for the tertiary implies that its profiles do not fall completely within those of the primary, but this effect is hardly visible outside the wings and below the noise level.

Finally, we note that the system contains two stars in the β Cephei instability strip (see, e.g., Pamyatnykh 1999). It is therefore very well possible that the tertiary also exhibits oscillations. Its larger rotational velocity will imply more smearing out of the oscillatory signature within the profiles and its lower flux will limit its contribution to the observed variability, but we have to keep in mind the possible contribution of the tertiary to the low-level line-profile variability (see Paper II).

7. Conclusions

We are now ready to synthesize all the results of our analyses and come up with a unique scenario for the multiple system λ Scorpii, after 14 years of spectroscopic monitoring. First of all, we have provided evidence for the early-B-type nature of the primary and the tertiary moving in an eccentric ($e = 0.23$) orbit of 2.96 years in complete agreement with the interferometric results of Hanbury Brown et al. (1974).

Berghöfer et al.'s (2000) interpretation of the secondary as an ultra-massive white dwarf has to be abandoned. It was based on the uncertain mass function found by De Mey et al. (1997), who did not have sufficient data to disentangle the orbital motion from the pulsational variability of the primary. While we found very similar values for the orbital period ($5\overset{\rm d}{.}9525$ days) and eccentricity ($e = 0.26$) of the short orbit to those of De Mey et al. (1997), the mass function has more than doubled in value. This implies a secondary with a mass largely above the Chandrasekhar limit, the most likely range being $M_2 \in [1.6, 2.0]\,M_\odot$.

Berghöfer et al.'s (2000) suggestion of a white dwarf companion was also based on the large $L_{\rm X}/L_{\rm bol}$-ratio of -6.74 of λ Scorpii derived by Cohen et al. (1997) and the softness of the X-ray excess. However, this $L_{\rm X}/L_{\rm bol}$-ratio is not so abnormally high. Cohen et al. (1997) find the same value for the binary β Cephei star β Centauri, which is composed of two equal B2 components (Ausseloos et al. 2002). It is true that λ Scorpii is the only B1.5 star with such a large soft X-ray excess, which Berghöfer et al. (2000) attributed to the secondary. They further argued that a (pre-) main-sequence star or a neutron star would give rise to much harder X-rays than the observed extreme soft X-rays. Although this statement is true for most (pre-) main-sequence and neutron stars, exceptions are known. Pavlov et al. (2002) reported the existence of neutron stars with soft X-ray spectra. An example of a neutron star with a similar X-ray flux as observed for λ Scorpii, which is the companion of the O-type subdwarf HD 49798, is given by Israel et al. (1997). According to Stella et al. (1986) the absence of hard X-rays induced by wind accretion in binary systems consisting of a neutron and an OB-type star can be naturally explained if the neutron star is very young and very rapidly rotating. In that case the spinning of the neutron star prevents the stellar wind from penetrating through the neutron star accretion radius such that all matter is expelled from the system. Also several main-sequence stars turn out to have soft X-ray fluxes according to Hünsch et al. (1998). We do reckon, however, that for these stars the X-ray fluxes are typically of order $L_{\rm X} \sim 10^{29}$ erg s^{-1} rather than $L_{\rm X} = 1.11 \times 10^{31}$ erg s^{-1} as is measured for λ Scorpii (Cohen et al. 1997). It therefore seems more likely that we are dealing with a pre-main-sequence secondary. Indeed, Alcalá et al. (1997) list three pre-main-sequence stars with hardness ratio below -0.5 pointing towards soft X-rays, in analogy to λ Scorpii. Moreover, Neushäuser et al. (1995, see their Fig. 7) find X-ray fluxes between 10^{30} and 10^{31} erg s^{-1} for a sample of weak T Tauri stars. Such stars have only very weak H_α emission which would not turn up in the spectrum of λ Scorpii because the contribution to the overall spectrum is two orders of magnitude below that of the primary.

The observed eclipses in the HIPPARCOS and ground-based photometric data argue against the neutron star scenario. The presence of a neutron star companion would have the additional complication that the triple system must have survived the mass loss from the system and the kick imparted to the neutron star during the supernova explosion in which it was formed. It is therefore most likely that the correct interpretation of the secondary of λ Scorpii is a weak-lined naked T Tauri star. We note, however, that from a theoretical point of view the formation of such a close system consisting of a B star and a naked T Tauri star is not straightforward. Aerts et al. (1999) found no IR excess for λ Scorpii from IRAS data which would be compatible with a naked T Tauri star. However, it would be interesting to perform IR observations with much higher resolution than IRAS to check if there is any evidence for the remnants of the proto-stellar disk. Also,

Table 4. Overview of the stellar parameters of the three components of the triple system λ Scorpii as derived in this paper. We list the mass, expressed in $M_\odot$, the effective temperature ([K]), the value of $\log g$ and the spectral type or nature of the star.

	Mass	$T_{\rm eff}$	$\log g$	
1	[10, 12]	[24 000, 26 000]	[3.7, 3.9]	B1.5IV
2	[1.6, 2.0]			pre-MS star
3	[8.6, 9.6]	[20 000, 22 000]	[3.9, 4.1]	B2V

XMM or Chandra measurements can give a definitive answer on the presence of a neutron star.

All the weak-lined T Tauri stars with $L_{\rm X}$ above 10^{30} erg s^{-1} in the sample of Neushäuser et al. (1995, see their Fig. 12) have ages between roughly 10^5 and 10^6 years, which is compatible with the assumption that the primary of λ Scorpii has passed less than half of its main sequence life and that the system belongs to the US OB2 association with an age near $\sim 6 \times 10^6$ years, as suggested by de Zeeuw et al. (1999). It is noteworthy that the study by the latter authors provides clear evidence for the occurrence of numerous pre-main-sequence stars in the close vicinity of λ Scorpii. Such a young age is also compatible with our results obtained from the population synthesis in the case of a detached system and gives a natural explanation of the eccentric orbit, even in the presence of resonant locking between dynamic tides and prograde gravity modes.

In summary we list the derived stellar properties of the three components of λ Scorpii in Table 4.

A first glance at the intrinsic variability of the primary of λ Scorpii by means of an analysis of the remaining radial velocity variations after correction for the orbital motion of the close and the wide system, confirmed the presence of a dominant frequency of $f_1 = 4.679410$ c d^{-1}. We have shown that this frequency is subject to the light-time effect within the wide orbit. A more detailed analysis of the frequency spectrum by means of the line-diagnostics is presented in Paper II. In this subsequent paper we also will investigate the possibility of a resonant excitation of the pulsation mode(s).

Acknowledgements. We thank Petr Hadrava and Petr Harmanec for putting the FOTEL code at our disposal and for various discussions. We also thank Jarrod Hurley, Onno Pols, and Chris Tout for sharing their analytical Single Star Evolution code and Ron Taam and Luigi Stella for useful discussions on the X-ray properties of young neutron stars. KU is supported by the Fund of Scientific Research – Flanders (FWO), project "G.0178.02". B.W. and U.K. acknowledge the support of the British Particle Physics and Astronomy Research Council (PPARC). BW also acknowledges the support of NASA ATP grant NAG5-13236 to Vicky Kalogera. K.L. and C.A. are much indebted to Joachim Puls for introducing them into the use of the latest version of FASTWIND and for the hospitality during their visits to Munich. K.L. is supported by the Research Fund K.U. Leuven under grant GOA/2003/04. Finally, we thank all the observers who contributed to the realisation of this long-term project: Christoffel Waelkens, Gwendolyn Meeus, Katrien De Mey, Coen Schrijvers, Koen Daems, Peter De Cat, Joris De Ridder, Caroline Van Kerckhoven, Wim De Meester, Roeland Van Malderen, Thomas Maas, Stephanie de Ruyter and Pierre Royer.

References

Aerts, C., De Pauw, M., & Waelkens, C. 1992, A&A, 266, 294
Aerts, C., De Mey, K., De Cat, P., & Waelkens, C. 1998, in A Half century of Stellar Pulsation Interpretation: A Tribute to Arthur N. Cox, ed. P. A. Bradley, & J. A. Guzik, ASP Conf. Ser., 135, 380
Aerts, C., De Boeck, I., Malfait, K., & De Cat, P. 1999, A&A, 347, 524
Alcalá, J. M., Krauter, J., Covino, E., et al. 1997, A&A, 319, 184
Baranne, A., Queloz, D., Mayor, M., et al. 1996, A&AS, 119, 373
Berghöfer, T. W., Vennes, S., & Dupuis, J. 2000, ApJ, 538, 854
Berghöfer, T. W., Schmitt, J. H. M. M., & Cassinelli, J. P. 1996, A&AS, 118, 481
Brown, A. G. A., & Verschueren, W. 1997, A&A, 319, 811
Buscombe, W. 1969, MNRAS, 144, 31
Cohen, D. H., Cassinelli, J. P., & MacFarlane, J. J. 1997, ApJ, 487, 867
Cowling, T. G. 1941, MNRAS, 101, 367
De Cat, P., & Aerts, C. 2002, A&A, 393, 965
De Mey, K., Aerts, C., Waelkens, C., et al. 1997, A&A, 324, 1096
De Zeeuw, P. T., Hoogerwerf, R., & De Bruijne, J. H. J. 1999, AJ, 117, 354
Eggleton, P. P., & Kiseleva-Eggleton, L. 2001, ApJ, 562, 1012
Erspamer, D., & North, P. 2002, A&A, 382, 227
Fitch, W. S. 1967, ApJ, 148, 481
Giacconi, R., Branduardi, G., Briel, U., et al. 1979, ApJ, 230, 540
Gulati, R. K., Malagnini, M. L., & Morossi, C. 1989, A&AS, 80, 73
Hadrava, P. 1990, Contr. Astron. Obs. Skal. Pl., 20, 23
Hadrava, P. 1995, A&AS, 114, 393
Hanbury Brown, R., Davis, J., & Allen, L. R. 1974, MNRAS, 167, 121
Handler, G., Balona, L. A., Shobbrook, R. R., et al. 2002, MNRAS, 333, 262
Harmanec, P., Hadrava, P., Yang, S., et al. 1997, A&A, 319, 867
Herrero, A., Puls, J., & Najarro, F. 2002, A&A, 396, 949
Heynderickx, D., Waelkens, C., & Smeyers, P. 1994, A&AS, 105, 447
Hoffleit, D. 1982, The Bright Star Catalogue, Yale University Observatory, New Haven, Connecticut, USA
Hünsch, M., Schmitt, J. H. M. M., & Voges, W. 1998, A&AS, 132, 155
Hurley, J. R., Pols, O. R., & Tout, C. A. 2000, MNRAS, 315, 543
Iben, I., Jr., & Tutukov, A. V. 1999, ApJ, 511, 324
Israel, G. L., Stella, L., Angelini, L., et al. 1997, ApJ, 474, L53
Kalogera, V. 1996, ApJ, 471, 352
Kato, S. 1974, PASJ, 26, 341
Kubát, J., Puls, J., & Pauldrach, A. W. A. 1999, A&A, 341, 587
Léhmann-Filhés, R. 1894, Astr. Nach., 136, 17
Lesh, J. R., & Aizenman, M. L. 1978, ARA&A, 16, 215
Lomb, N. R., & Shobbrook, R. R. 1975, MNRAS, 173, 709
Neuhäuser, R., Sterzik, M. F., Schmitt, J. H. M. M., Wichmann, R., & Krautter, J. 1995, A&A, 297, 391
Pamyatnykh, A. A. 1999, Acta Astr., 49, 119
Pasinetti Fracassini, L. E., Pastori, L., Covino, S., & Pozzi, A. 2001, A&A, 367, 521
Pavlov, G. G., Zavlin, V. E., Sanwal, D., & Trümper, J. 2002, ApJ, 569, L95
Perryman, M. A. C., Lindegren, L., Kovalevsky, J., et al. 1997, A&A, 323, L49
Reyniers, K., & Smeyers, P. 2003a, A&A, 404, 1051
Reyniers, K., & Smeyers, P. 2003b, A&A, 409, 677

Roberts, D. H., Lehar, J., & Dreher, J. W. 1987, AJ, 93, 968
Santolaya-Rey, A. E., Puls, J., & Herrero, A. 1997, A&A, 323, 488
Scargle, J. D. 1982, ApJ, 263, 835
Schrijvers, C., & Telting, J. H. 2002, A&A, 394, 603
Shobbrook, R., & Lomb, N. R. 1972, MNRAS, 156, 181
Slipher, V. M. 1903, Lick. Obs. Bull., 1, 23
Smeyers, P., Willems, B., & Van Hoolst, T. 1998, A&A, 335, 622
Smith, M. A. 1985a, ApJ, 297, 206
Smith, M. A. 1985b, ApJ, 297, 224
Stella, L., & White, N. E. 1986, ApJ, 308, 669
Stellingwerf, R. F. 1978, ApJ, 224, 953
Stoeckley, T. R., & Buscombe, W. 1987, MNRAS, 227, 801
Taam, R. E., & Sandquist, E. L. 2000, ARA&A, 38, 113
Telting, J. H., Abbott, J. B., & Schrijvers, C. 2001, A&A, 377, 104
Trümper, J. 1983, Adv. Space Res., 2(4), 241
Uytterhoeven, K., Telting, J. H., Aerts, C., & Willems, B. 2004, A&A, 427, 593 (Paper II)
Waelkens, C. 1990, in Angular Momentum and Mass Loss for Hot Stars, ed. L. A. Wilson, & R. Stalio, 235
Watson, R. D. 1971, Ph.D. Thesis, Mount Stromlo Observatory
Watson, R. D. 1988, Ap&SS, 140, 255
Westin, T. N. G. 1985, A&AS, 60, 99
Willems, B., & Aerts, C. 2002, A&A, 384, 441
Willems, B., & Kolb, U. 2002, MNRAS, 337, 1004
Willems, B., & Kolb, U. 2004, A&A, 419, 1057
Witte, M. G., & Savonije, G. J. 1999a, A&A, 341, 842
Witte, M. G., & Savonije, G. J. 1999b, A&A, 350, 129
Zahn, J.-P. 1992, in Binaries as Tracers of Stellar Formation, ed. A. Duquennoy, & M. Mayor (Cambridge: Cambridge Univ. Press), 253

Online Material

Table 1. Journal of the observations of λ Scorpii measured during the period May 1988–July 2002. The columns list the month and year of the observations, the number of spectra obtained and the range in signal-to-noise (S/N) ratio. The spectra were reduced following the schemes outlined in Sects. 3.1 and 3.2 (indicated by * and $^\circ$ respectively). The bottom part is a logbook of the 421 spectra obtained during the period 20–28 July 1997. The columns list the Julian date of the observations, the number of spectra obtained, the mean S/N and the mean integration time expressed in seconds.

Month	Year	N	S/N range
May	1988	12	400–700
June	1995	191	150–350
March	1996	13	300–400
April	1996	27	350–600
May	1996	2	300
June	1996	10	150–200
July	1996	12	150–350
March*	1997	5	400–500
May*	1997	11	500–750
July*	1997	421+5	400–650
October*	1997	3	350–400
February$^\circ$	2001	18	100–250
April$^\circ$	2001	21	50–150
July$^\circ$	2001	29	50–130
February$^\circ$	2002	5	140
March$^\circ$	2002	9	50–150
July $^\circ$	2002	21	50–200
Date (HJD)	N	S/N	Δt (s)
2 450 650	59	552	75
2 450 651	31	515	145
2 450 652	70	601	60
2 450 653	59	608	77
2 450 654	52	620	82
2 450 655	52	580	64
2 450 656	47	537	70
2 450 657	49	558	90